Estimation of Wind Turbine Radar Signature at 13.5 MHz

Calvin C. Teague and Donald E. Barrick
CODAR Ocean Sensors, Ltd.
1914 Plymouth Street, Mountain View, CA 94303
Email: cal@codar.com, don@codar.com

***Abstract*—The radar cross sections (RCS) and frequency spectra of a wind turbine consisting of three conducting blades of 42 m radius, with a vertical mast of 65 m over a perfect ground plane, was estimated using the Numerical Electromagnetics Code (NEC). The NEC input deck generation, parsing the NEC output to select the RCS numbers, plotting the time series, and calculating and plotting the frequency spectra were all done by bash shell scripts. The shell scripts generally set up several environment variables and then called Ruby, Octave or Gnuplot programs to perform the text manipulations, data calculations and plot generation. Calibrated plots of time series and frequency spectra for several cases are included. The effect of a dielectric blade is briefly considered.**

I. Introduction

As offshore wind turbines are developed and deployed, high-frequency (HF) radar networks are being installed to aid in planning and operating large wind farms. In addition, wind farms are being planned or installed in existing HF radar coverage areas. However, the potential exists for interference to the HF radar operation from the turbines. The rotation rate of the turbine blades is comparable to the Doppler shift due to the wave motion which is sensed by the radar, and the physical size of the rotating blades is comparable to the wavelength used by the radars. This paper presents a summary of a study done to estimate the radar cross section (RCS) and the resulting frequency spectrum of a turbine with three 42-m conducting blades at a radar frequency of 13.5 MHz. The simulations were also run for 4.5 MHz and 25.4 MHz to examine the frequency behavior.

II. Method

The radar cross section was estimated using the Numerical Electromagnetics Code (NEC) computer program [1], a program used for several decades to calculate antenna radiation patterns. With the appropriate input parameters, it can also calculate the radar cross section of an arbitrary structure.

A. NEC Model

A turbine with three blades, a mast, and a generator structure was modeled by wires as sketched in Fig. 1, and the blade structure was rotated through 120° in 5° steps to study the effects of the blade rotation. Because of the 3-fold blade symmetry, the RCS time series repeats after a rotation of 120°. Referring to a Wikipedia article describing the Hywind turbine near Stavanger, Norway [2], a blade length of 42 m and a tower height of 65 m were used in this study, with 20 segments for each blade and 50 segments for the mast. The radar cross section was calculated with and without the mast, in free space and over a perfect ground plane, and for four different aspect angles in 30° steps, ranging from looking face-on to edge-on with respect to the blades. Although the results are for these specific parameters, the procedure can be extended easily to accommodate other radar frequencies or turbine dimensions.

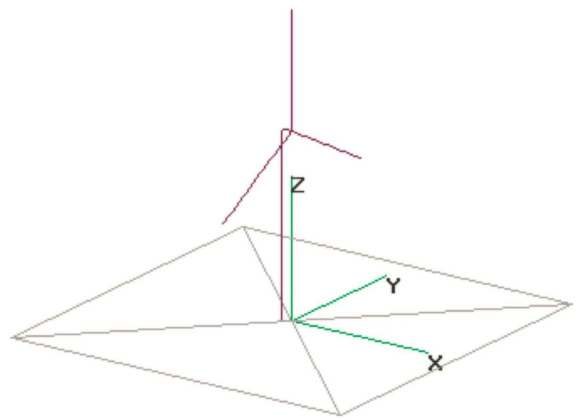

Fig. 1. NEC model of a 3-blade turbine with three 42-m blades offset 3.5 m from a 65-m mast over a perfect ground plane. The turbine spin axis is parallel to the *x*-axis. The aspect angle ϕ is measured from the *x*-axis.

B. NEC Output Processing

The NEC output was processed by a Ruby script. Each NEC output file (one for each aspect angle ϕ) contained information for blade rotation angles from 0° through 120°. The script searched through the NEC output, identifying each section from the COMMENTS header, and extracted the blade rotation angle, and then looked for the RADIATION PATTERNS header and extracted the RCS and phase angle information. The information was written to an output file for subsequent processing.

C. NEC calibration

When generating pattern information using a plane wave excitation, NEC reports a "gain" value which is really the RCS in dB relative to wavelength squared. In order to calculate a spectrum, an equivalent "voltage" was calculated as $v = 10^{(dB/20)} \exp(i\alpha)$, where α is the phase angle from the tenth field of the RADIATION PATTERNS output. Thus v is a complex quantity. It has units of meters/wavelength (dimensionless) and was included in the output of the NEC output parsing script. The magnitude of v was plotted as a time series of $\sqrt{RCS} = |v|\lambda$ with units of meters, where λ is the radar wavelength. The quantity v (complex) was used as input to an FFT calculation of the frequency spectrum, whose "voltage" coefficients were also in units of meters.

D. Octave FFT calibration

The spectrum of the turbine signal was calculated using Octave [3]. By feeding controlled inputs to the Octave FFT routine, it was determined that an FFT of N DC samples of unit amplitude resulted in a DC output of N. A unit-amplitude single-cycle cosine wave of N points exactly spanning the input buffer resulted in FFT outputs at frequency bins ± 1 of $N/2$ each. Consequently, when processing the NEC RCS time series data of length N, the FFT output was multiplied by λ/N to get frequency-bin coefficients s in units of meters. These were then converted to dBsm using $dBsm = 20\log_{10}(s)$. For all cases plotted here, $N = 24$ with a rotation step size of $5°$. The time series was exactly periodic in 24 samples, so no window was needed to avoid spectral leakage between FFT bins.

III. Behavior at 13.5 MHz

The study concentrated on 13.5 MHz because a wind turbine installation is currently underway on the east coast of the U.S. in the field of view of a 13.5-MHz SeaSonde system.

A. Time Series

Figure 2a below shows an example of $\sqrt{RCS}$ as a function of rotation angle; $\sqrt{RCS}$ is proportional to the voltage seen by the radar and is used in the calculation of the RCS spectrum. While the variation with rotation angle is smooth when the turbine is seen face-on, much sharper features are seen when the turbine is viewed edge-on. Consequently the spectrum of the turbine signal will likely contain several significant harmonics. Figure 2b shows the Fourier transform of these signals. The horizontal axis is shown as harmonic number to allow for different turbine rotation rates, although it is expected that operationally the turbine rotation rate, and the frequencies of the harmonics, is tightly controlled, resulting in very narrow spectral lines for a time series extending over several minutes. For a typical 3-blade rotation rate of 15 rpm [4], harmonic number 1 corresponds to 0.75 Hz, harmonic number 2 corresponds to 1.50 Hz, etc. While most of the energy in the face-on spectrum is at DC, for the other aspect angles there is significant energy in at least 3 or 4 harmonics (up to at least 3 Hz), and possibly even higher. The RCS in these harmonics is on the order of 30 dBsm.

B. Radar Cross Section

For comparison, the total radar cross section of a 3-km wide ocean semicircle at a range of 15 km is about 61.5

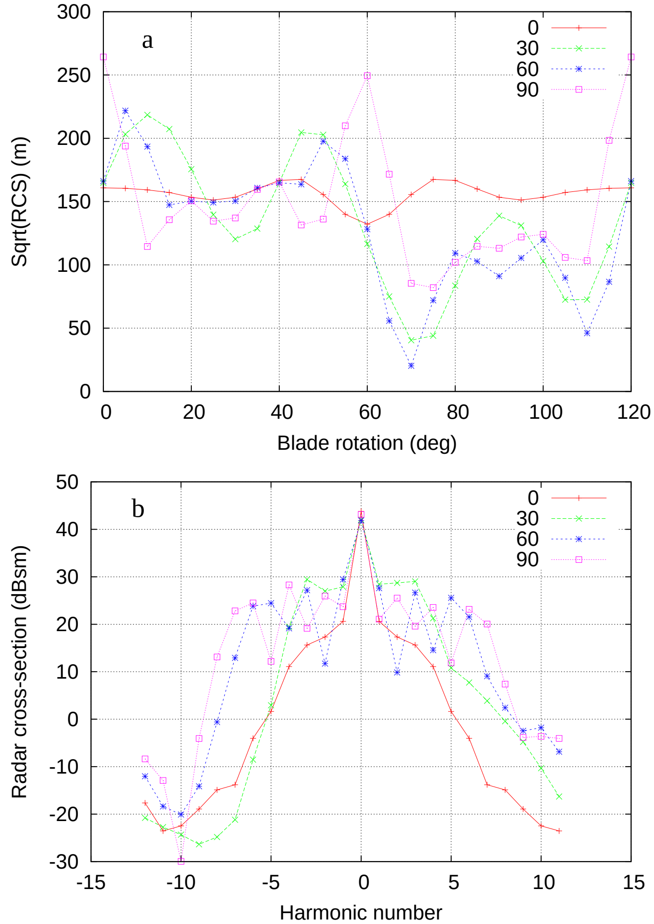

Fig. 2. Time series (a) and spectra (b) of a turbine signal with three 42-m blades 3.5 m from a 65-m mast and with a center of rotation at 65 m over a perfect ground plane at 13.5 MHz. The time series plot covers $120°$ of turbine rotation. Four aspect angles are shown: $\phi = 0°$ corresponds to viewing the blades face-on, $\phi = 90°$ corresponds to viewing them edge-on. The frequency axis in the spectral plot is harmonic number. Harmonic number 1 corresponds to one cycle per $120°$ of turbine rotation (0.75 Hz for 15 rpm, 0.50 Hz for 10 rpm).

dBsm, and if this energy is spread into 20 Doppler bins, the energy in each bin is about 48.5 dBsm. Thus the energy in the turbine harmonics may be 18 dB below the peak Bragg energy. However, the weaker ocean Bragg (approaching/receding) line may be 10–20 dB below the stronger line, so the turbine energy may be comparable to the weaker Bragg energy, and it could be comparable to the second-order energy even for the stronger line. For a shorter range, say 5 km, the area of the ocean semicircle, and hence its radar cross section, would be smaller, while the turbine RCS remains the same, so the turbine signal relative to the ocean signal (assuming that the turbine is at the shorter range) would be even stronger.

IV. Additional Configurations

A. Ground Plane, Mast

When the calculations were repeated without a ground plane, the RCS was lower by a factor of about 16 (-12 dB). Although operation without a ground plane is not realistic, the

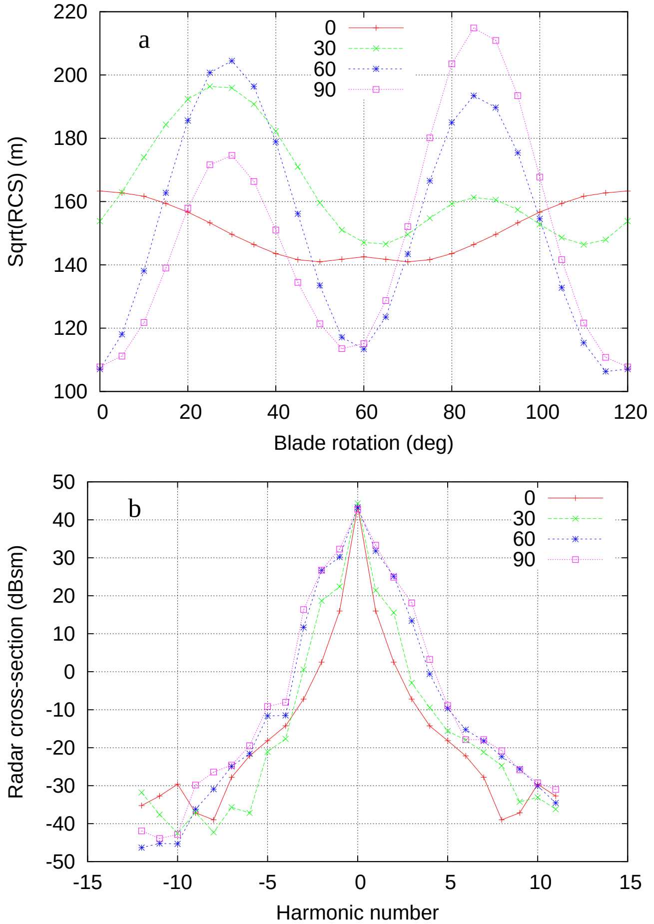

Fig. 3. Time series (a) and spectra (b) of a turbine signal with three 42-m blades 3.5 m from a 65-m mast and with a center of rotation at 65 m over a perfect ground plane at 4.5 MHz. The time series plot covers 120° of turbine rotation. Four aspect angles are shown: $\phi = 0°$ corresponds to viewing the blades face-on, $\phi = 90°$ corresponds to viewing them edge-on. The frequency axis in the spectral plot is harmonic number. Harmonic number 1 corresponds to one cycle per 120° of turbine rotation (0.75 Hz for 15 rpm).

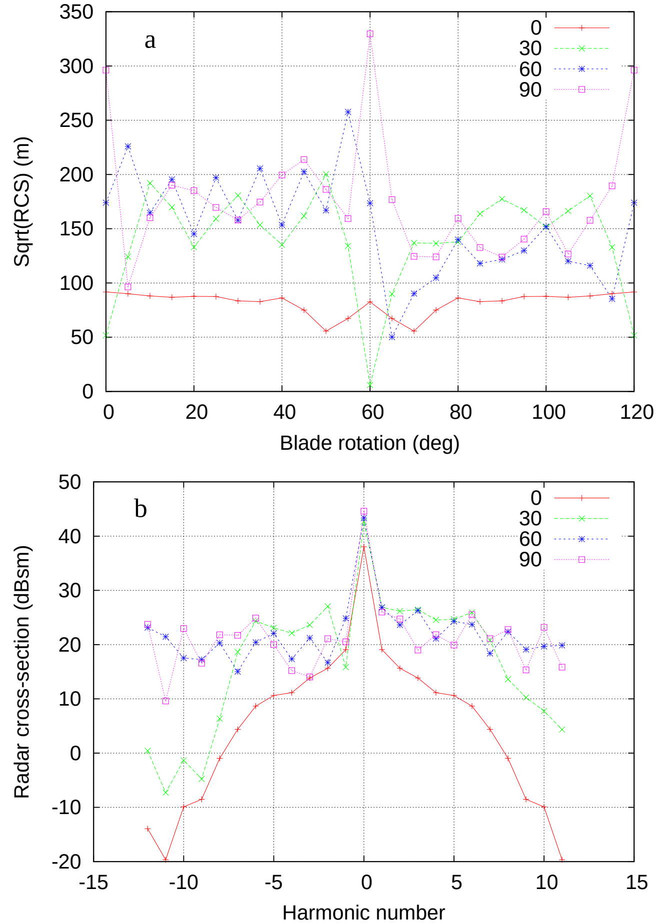

Fig. 4. Time series (a) and spectra (b) of a turbine signal with three 42-m blades 3.5 m from a 65-m mast and with a center of rotation at 65 m over a perfect ground plane at 25.4 MHz. The time series plot covers 120° of turbine rotation. Four aspect angles are shown: $\phi = 0°$ corresponds to viewing the blades face-on, $\phi = 90°$ corresponds to viewing them edge-on. The frequency axis in the spectral plot is harmonic number. Harmonic number 1 corresponds to one cycle per 120° of turbine rotation (0.75 Hz for 15 rpm).

observed change was what was expected. When the mast was omitted, the spectra were more symmetrical around DC (note the slight asymmetry in the spectrum for $\phi = 30°$ in Fig. 2b). Again, operation without a mast is not realistic, but apparently the presence of the mast introduces some phase shifts which can affect the spectral symmetry around DC.

B. 4.5 MHz

The calculations were repeated for 4.5 MHz. The resulting time series is shown in Fig. 3a. Comparing this with the time series at 13.5 MHz in Fig. 2a, it is clear that the waveform is much smoother as a function of rotation angle, and the spectrum in Fig. 3b has much lower energy in the higher harmonics than at 13.5 MHz. The magnitude of the time series, and of the lower-order harmonics, is similar for the 13.5-MHz case.

C. 25.4 MHz

The calculations were also repeated for 25.4 MHz, using 40 segments for the blade wire and 60 for the mast, to keep the segment size less than 0.1 wavelength. The resulting time series is shown in Fig. 4a. As expected from the previous plots, the time series has much sharper features than for the lower frequencies, and the spectrum in Fig. 4b contains more energy in the higher harmonics. Again, the magnitude of the time series and of the lower-order harmonics is similar to the other cases.

D. Blade Material

The NEC simulations above were carried out using a conducting wire model for the blades and mast. However, the blades of large wind turbines may be constructed of non-conducting material, such as Fiberglass-reinforced epoxy [4]. Unfortunately, there is no convenient way to model dielectric structures directly in NEC. A rough estimate of the effect of the dielectric material may be made in a couple of ways.

First, consider electric field reflection from a flat surface at normal incidence. For a perfectly conducting surface, the reflection coefficient $R = 1$. For a dielectric surface with dielectric constant ε,

$$R = \frac{\sqrt{\varepsilon}-1}{\sqrt{\varepsilon}+1}$$

Fiberglass has a dielectric constant $\varepsilon \approx 4.5$, so $R = 0.359$, or -8.9 dB compared to that of a perfect conductor.

Alternatively, consider the scattering width σ of an infinitely-long circular cylinder at normal incidence with radius a and wavenumber k_0 [5]. (The scattering width is the counterpart of the RCS when scattering is two dimensional as it is for infinitely long cylinders.) For a perfectly conducting cylinder,

$$\sigma_c = \frac{\pi a^2}{k_0 a \left[\ln^2(0.8905 k_0 a) + \frac{\pi^2}{4}\right]}$$

For a dielectric cylinder,

$$\sigma_d = \pi a \frac{\pi}{4} (k_0 a)^3 \left|\varepsilon - 1\right|^2$$

In both cases, it is assumed the E-field is parallel to the cylinder axis.

To illustrate the difficulty in defining a model for the dielectric blade, consider the following: The NEC simulations were done using a wire radius of 0.2 m. Taking $a = 0.2$ m and $\lambda = 22.2$ m (13.5 MHz), then $k_0 a = 0.0565$, and the ratio of the radar scattering widths is $0.00109/0.195 = 0.0056$ or -22 dB. Reference to a picture of a 75-m blade in its mold [6] suggests that a larger equivalent radius might be more realistic, even for a 42-m blade. If the radius of the dielectric rod is increased to 1.0 m, then the value of σ_d for the dielectric material is 0.683 and the ratio of the 1.0-m radius dielectric σ_d to the 0.2-m radius conductor σ_c is $0.683/0.195 = 3.5$ or $+5.4$ dB. However, the fiberglass blade in [6] is hollow, which will decrease its radar cross section compared to a solid rod. But if there are any wires inside the fiberglass, for sensors or warning lights, or if the surface is conductive due to wet salt spray or other coating, the structure will act more like a wire conductor.

Without more information about the blade material, it really is impossible to predict the magnitude of the dielectric turbine cross section, but it could be significant. However, the waveform shape and time series harmonic content is likely to be similar to that estimated for the conducting wire model.

V. Discussion

The frequency of the Bragg ocean signal is between 0.228 and 0.669 Hz for radar frequencies between 5 and 43 MHz, so at first glance the turbine and ocean signals appear to be separated in frequency. However, the narrow turbine lines may overlap the ocean energy because of aliasing. Coastal radars typically sample the (complex) Doppler time series at a rate of 1.0 or 2.0 Hz, so signals above the Nyqist frequency will be aliased, perhaps multiple times, and folded into adjacent range bins due to the range-Doppler coupling of the FMCW waveforms typically used. Anti-aliasing filters are really not possible with the waveforms currently used, so depending on the radar repetition rate, turbine rotation rate and turbine aspect angle (which will change depending on wind direction), some of the turbine lines may overlap the ocean signals. This effect can be mitigated by using higher sweep rates, but this may decrease the number of GPS-synchronized radars which can be accommodated in a given area. Given the lack of information regarding the structure and typical operating parameters of proposed wind turbine installations, detailed field experiments should be conducted to study the wind turbine influence on coastal HF radars.

References

[1] *NEC-2 Users Manual, Part 3*, http://users.commspeed.net/k7qo.

[2] *Hywind turbine*, http://en.wikipedia.org/wiki/File:Hywind.jpg.

[3] *Octave*, http://www.gnu.org/software/octave/.

[4] *Siemens Wind Turbine SWT-2.3-82 VS Product Brochure*, Siemens AG, 2009, Available at http://www.energy.siemens.com/hq/en/power-generation/renewables/wind-power/.

[5] George T. Ruck, Donald E. Barrick, William D. Stuart, and Clarence K. Krichbaum, *Radar Cross Section Handbook*, Plenum, 1970, pp. 213 and 223.

[6] *Siemens Wind Turbine SWT-6.0-154 VS Product Brochure*, Siemens AG, 2011, Available at http://www.energy.siemens.com/hq/en/power-generation/renewables/wind-power/.